

Evolution of the void structure in plasma-sprayed YSZ deposits during heating^a

Jan Ilavsky^{a,*}, Gabrielle G. Long^a, Andrew J. Allen^a, Christopher C. Berndt^b

^a National Institute of Standards and Technology, Gaithersburg, MD, USA

^b Center for Thermal Spray Research, State University of New York at Stony Brook, Stony Brook, NY, USA

Abstract

The evolution of the anisotropic void microstructure of plasma-sprayed yttria-stabilized zirconia (YSZ) deposits has been observed as a function of temperature by small-angle neutron scattering. Scattering experiments were carried out *in-situ*, in a furnace between 600 and 1400°C. The terminal slope (Porod scattering) of the scattering spectra was used to derive the specific surface area of the voids. For samples with sufficient scattering anisotropy, the two major void systems — intersplat (inter-lamellar) pores and intrasplat cracks — could be characterized separately. The pore and crack specific surface areas were found to depend on temperature differently. The specific surface area of the intrasplat cracks decreased markedly at temperatures below 1000°C, whereas the specific surface area of the intersplat pores began to decrease above 1000°C. This indicates important differences in the sintering of these two void systems probably related to their size and shape. Changes in the void surface were observed at temperatures as low as 800°C, a temperature comparable to, or less than, the usual operational temperature for this material. © 1999 Published by Elsevier Science S.A. All rights reserved.

Keywords: Thermal-spray deposits; Small-angle scattering; Sintering; Yttria-stabilized zirconia; Neutron scattering; Thermal barrier coatings

1. Introduction

Plasma-sprayed yttria-stabilized zirconia (YSZ) (8 wt.% Y₂O₃ in ZrO₂) deposits currently find application in the hot sections of power operating systems, such as on turbine blades [1–4]. They serve as thermal barrier coatings which reduce the temperature of the metallic (structural) components and, therefore, allow either the operating temperature to be increased [5] (which improves engine efficiency) or the lifetime of components to be extended [6,7] (which reduces maintenance cost). These coatings are exposed to severe conditions as they carry out their functions. They must survive repeated heating cycles between ambient and operating temperatures of 1100–1400°C. They are also exposed to hostile environments which cause erosion and corrosion [8,9], the severity of which depends on the microstructure of the coatings.

Some changes in the microstructure of the coatings should be expected under the severe operational conditions of thermal barrier coatings. Up to now, a major focus of research has been on lifetime predictions under various operating conditions for coatings made of different materials [10–14]. However, few studies have characterized specific property (such as microstructural) changes during the life cycle. A major problem is that the operational conditions are so severe that they cannot be reproduced easily in the laboratory.

Changes during the life cycle suggest that there is an evolution of the microstructure, the chemistry, the residual stress distribution, the phase content, and other parameters that describe the state of engineering parts [15,16]. To improve current understanding, it is necessary to identify the influence of in-service parameters with respect to a limited number of properties. Ideally, the microstructural processes studied should be independent of each other. However, despite the fact that the temperature dependence of the void structure in plasma-sprayed alumina involves a combination of sintering and phase transformations [17], the temperature dependence of the void microstructure in YSZ deposits

*This paper is dedicated to Professor Herbert Herman on the occasion of his 65th birthday.

*Corresponding author. Tel.: +1-630-252-0866; fax: +1-630-252-0862.

E-mail address: ilavsky@aps.anl.gov (J. Ilavsky)

is nearly independent of phase changes in the mostly tetragonal YSZ deposits [18].

The microstructure of the as-sprayed zirconia deposit is dominated by three major void systems: intersplat pores and intrasplat cracks, each possessing preferred orientations [19,20], and globular voids. Intersplat pores are mostly parallel to the substrate and are formed between the lamellae during deposition. The intrasplat cracks are mostly perpendicular to the substrate and are formed either during cooling of the lamellae after solidification or at a later time, and are associated with stress relief [21]. Previous work has indicated a higher surface area for intersplat pores and a lower surface area for the intrasplat cracks [22] in some YSZ deposits. For alumina deposits, the surface areas of these two void systems are approximately equal, or the intrasplat crack surface area may dominate depending on the spray process. The surface area of the globular pores represents a small isotropic contribution to the voids surface area and is not, therefore, discussed in this paper.

This paper presents in-situ small-angle neutron scattering (SANS) studies of the microstructural evolution of the void structure of YSZ plasma sprayed deposits that occurs during heating of the deposit between room temperature and 1400°C. Earlier work [23] has shown that the microstructure of these materials changes substantially during the first thermal cycle. These changes are usually more severe than those in subsequent cycles, except, when long term migration of yttria causes a loss of phase stabilization [24].

2 Experiment

2.1. Sample manufacture

Plasma-sprayed deposits were produced by a Plasma Technik F4*, Sulzer Metco plasma-spray system. The spray-nozzle diameter was 8 mm, the powder injector diameter was 1.8 mm, and the current was 500 A at 68 V. The powder feed rate was 26 g min⁻¹ with 40 slpm (liters per minute at standard pressure and temperature) argon primary gas and 10 slpm hydrogen secondary gas, with 3 slpm argon carrier gas. The feed stock material was Amdry 142' (Alloy Metals) ZrO₂ + 8 wt.% Y₂O₃ powder of +41–113 μm particle size. This powder was produced by the fused-and-crushed method [18]. The torch-to-substrate distance was 90 mm. To obtain free-standing samples for this study, deposits of

about 5 mm thickness were sprayed onto a mild steel substrate (50 x 25 x 2.5 mm) which was pre-coated with a thin (<0.1 mm) layer of arc-sprayed aluminum. After YSZ deposition, the Al layer was dissolved in 20% HCl to obtain free-standing deposits. A low-speed (lubricated) diamond saw was used to section the samples to 25 x 5 x 5 mm thick.

2.2. Experimental procedure

SANS was employed to follow the evolution of the microstructure within the deposits. This technique has been used by the authors in previous studies to characterize ex-situ deposit void microstructures [25]. The present measurements are the first SANS measurements of this system performed in-situ in a high-temperature furnace [26].

The SANS technique that was used is an anisotropic variation of Porod scattering [25,27–29], which can be used to characterize the scatterers (i.e. the voids in this case) by their surface areas [30] without the need to know the sample porosity; provided the skeletal density is known. For isotropic materials, the surface area derived from Porod data in any direction is a quantitative specific surface area of the void microstructure. For anisotropic materials, the specific surface area result in any particular direction is actually an apparent Porod surface that must be mathematically related to the true void surfaces. To obtain a quantitative result for anisotropic materials it is necessary to measure the scattering from the sample in all directions (i.e. over 4π steradians). Fortunately the microstructure of the present deposits is circularly-symmetric when viewed from the top (perpendicular to the substrate), and only anisotropic in the two orthogonal directions. Furthermore, the anisotropy is the same in these two orthogonal directions. Thus, a measurement of the distribution of scattering from one cross section (plane perpendicular to substrate) is sufficient to derive the scattering in all directions.

A typical 3-dimensional (3-D) distribution of apparent Porod surfaces in plasma sprayed deposits is a bulging ellipsoid, such as the one shown in Fig. 1. The 3-D integral over this apparent Porod surface distribution can be used to derive quantitatively the specific surface area of all voids in the microstructure, even though the apparent specific surface area in any one direction does not necessarily reflect the true distribution of surface area in that direction.

Only one Porod scattering range can be discerned (Fig. 2a) for any sample. This is because all of the dimensions in each of the void components are too large to give anything but a single Porod scattering slope in the scattering regime studied. However, the two dominant planar void systems (cracks and lamellar pores) have significantly different orientational distribu-

¹ Certain trade names and company products are identified in order to adequately specify the experimental procedure. In no case does such identification imply recommendation or endorsement by the National Institute of Standards and Technology, nor does it imply that the products are necessarily the best for the purpose.

tions, as mentioned above, and their Porod scattering contributions can be separated by considering the orientational variation of the total Porod scattering intensity (Fig. 2b). The bulging ellipsoid surface distribution can be decomposed into two components, as shown in Fig. 1: a prolate shaped distribution (approximately ellipsoidal) that can be associated with the surface areas of the intersplat pores; and an oblate-shaped distribution that can be associated with the surfaces of the intrasplat cracks. Provided each void system distribution is sufficiently (and differently) anisotropic, each system can be evaluated separately because the scattered intensities from the individual void populations add linearly. As noted above, the surface area of the globular pores cannot be discerned in this experiment.

It should be noted here, that a description of the 3-D distribution of apparent Porod surfaces as ellipsoids is an approximation. A more detailed study by the authors shows that the proper shapes are more complex. In particular, for intersplat planar pores oriented with their plane normal more than about 45° from the spray direction, a prolate cylindrical apparent Porod surface distribution was found to be more appropriate than a prolate ellipsoid. Similarly, for intrasplat cracks oriented with their plane normal more than about 45° out of the substrate plane, an oblate cylindrical (plate-like) apparent Porod surface distribution was found to be more appropriate than an oblate ellipsoid. The use of

these more exact shapes in the evaluation results in small changes in the surface ratios of the two void systems, but the overall trends are the same. The derivation of the shape analysis is beyond the scope of this paper. The results shown in Fig. 3 make use of the more complex function, although we will continue to refer to the shapes in the 3-d figures as ellipsoids. Fig. 3 omits the small surface area attributable to the globular pores. Although the globular pores contribute little to the total surface area, it should be emphasized that their contribution to the overall porosity is significant.

The SANS characterization of void systems by means of their surface area brings to the field of plasma-sprayed deposits a quantitative result which represents the specific total surface areas of each void system. The following example illustrates this method of characterization of the void system by means of specific surface area, and shows the strengths and limitations of this method. A simple model for the roughly spherical voids observed within lamellae of these deposits is as follows: assuming the voids are spheres of the same size, their specific surface area can be calculated as $S = 3\phi/r$, where ϕ is their fractional volume (i.e. 0.1 for 10% porosity) and r is the void radius. A 10% porosity composed of 1 μm radius spherical voids has a specific surface area of 0.3 m²/cm⁻³ (or 3000 cm² cm⁻³ (or 3000 cm⁻¹)). Similarly, one can calculate the specific surface areas for other simply shaped voids, as well as

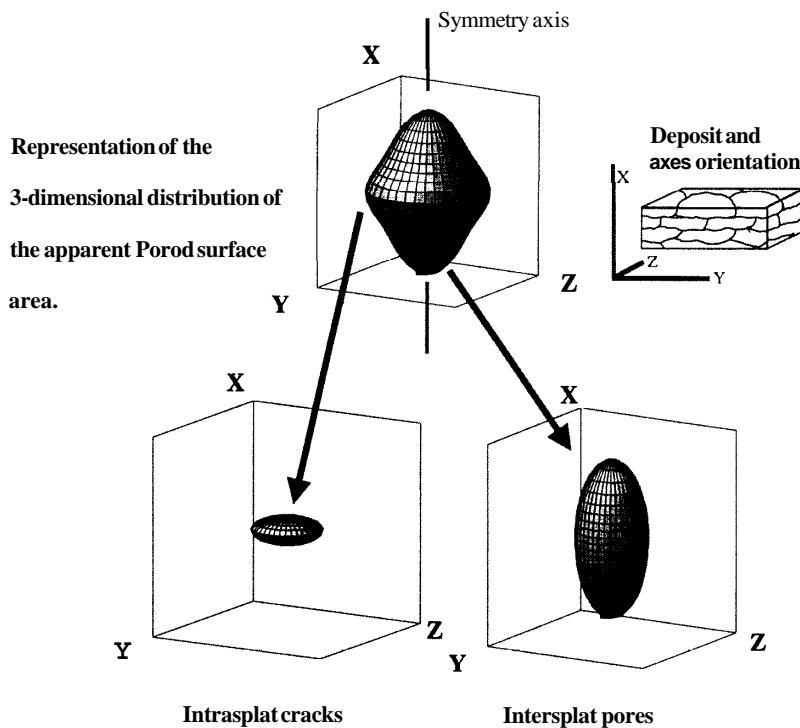


Fig. 1. 3-D distributions of apparent Porod surfaces for as-sprayed YSZ deposit. The upper figure shows the measured data that can be separated to show separate distributions for intrasplat cracks (left) and intersplat pores (right). Note that the zero in apparent Porod specific surface area is in the middle of each axis, and all three axes in each figure have the same scale. The values and labels are omitted for clarity.

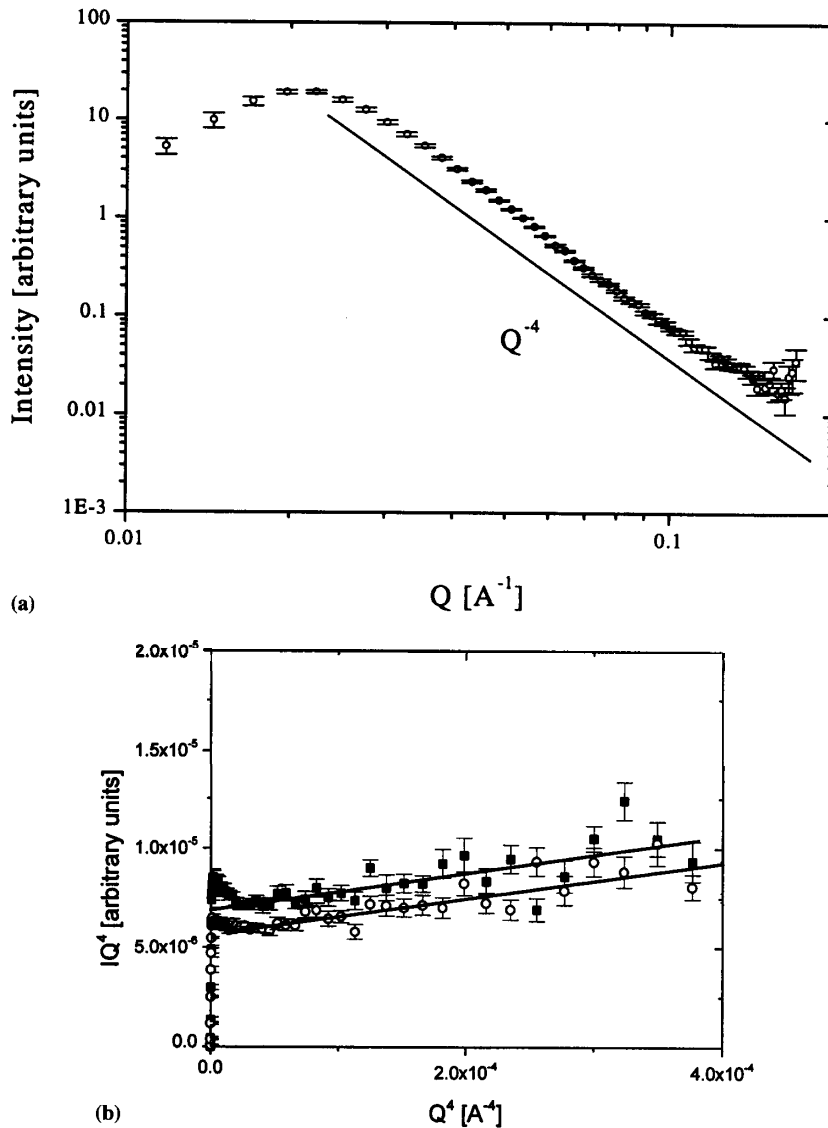


Fig. 2. (a) Log-log plot of intensity vs. Q . Only one Porod scattering regime (data parallel with the Q^{-4} line) is observed in the measured Q range. (b) IQ^4 vs. Q^4 plots evaluated with scattering vector (Q) parallel with the substrate (circles) and scattering vector perpendicular to the substrate (squares). The different intercepts of the fitted lines with the y-axis indicate differences in apparent Porod surface area for these directions.

for distributions of void sizes with a more complex formula for surface area. However, for shapes with higher aspect ratios the surface-to-volume ratio increases significantly.

The measured specific surface areas of the present deposits are about an order of magnitude higher than that expected from spherical voids. Thus, while crack-like voids with high surface-to-volume ratio are easily observed, roughly spherical voids are difficult to observe in the presence of extreme-shaped voids by means of this characterization method, even when these roughly spherical voids may contain a significant fraction of the total porosity. It also follows that the characterization of the voids by their surface area is incomplete. Since the sizes and shapes of the voids are generally unknown, a change in the surface area may

not reflect a similar change in their volume. For example, spheroidization of the very extreme shape of the voids may cause a significant reduction in surface area, even though their volume may not change at all.

2.3. Furnace experiment

The operating range of the SANS furnace [26] is between 600°C and 1700°C with a temperature homogeneity in the sample area controlled by this three-zone furnace to $\pm 5^\circ\text{C}$.

The neutron beam passes into the furnace through a single-crystal sapphire window. The beam then passes through the sample and exits through another single-crystal sapphire window. By suitable programming of the temperature profile, it is possible to model (with

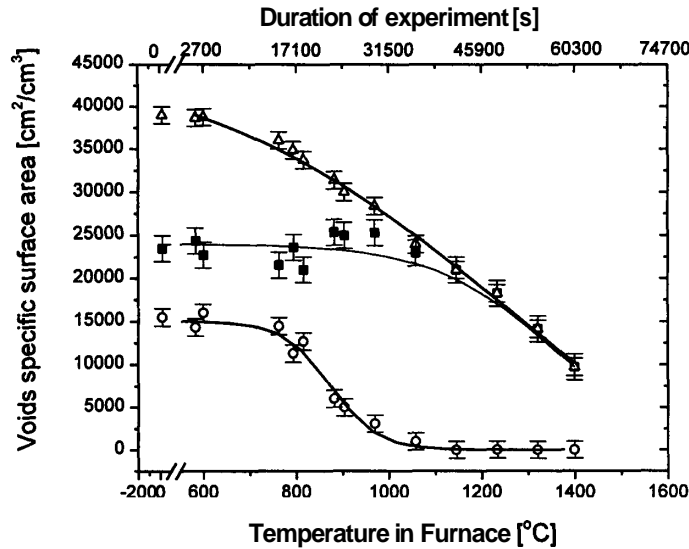


Fig. 3. Specific surface areas of void systems-dependence on time and temperature. Data symbols: the triangles represent total specific void surface area, the squares represent the specific surface area of the interlamellar pores and the circles specific surface area of the intralamellar cracks.

some limitations on heating and cooling rates) thermal cycles similar to those of in-service applications. The atmosphere in the furnace can be controlled and varied as needed. In the current experiment the atmosphere was nitrogen. Scattering by the sapphire windows was taken into account by means of intensity calibration and background subtraction following standard SANS data reduction procedures [27].

The sample was mounted in the furnace at room temperature and the first SANS spectrum measured. Then the furnace was heated rapidly ($800^{\circ}\text{C h}^{-1}$) to 600°C and held for about 0.7 h during which time the sample was measured again. These two SANS spectra were identical, indicating that no measurable changes had occurred in the microstructure. The sample was then measured continuously as the temperature was increased from 600 to 1400°C at $50^{\circ}\text{C h}^{-1}$. Data were collected continuously in 10 min intervals. Therefore, each spectrum contained data integrated over about a 8.8°C temperature interval. The average temperature in the interval was then assigned to the measured data. Finally, the furnace was cooled to room temperature and the sample was measured once more. This final spectrum agreed, within statistical error, with the last spectrum at 1400°C , indicating that no further microstructural changes had occurred during the cooling process.

3. Results

The total surface area of the voids decreased continuously above 600°C , as shown in Fig. 3, and, as indicated above, there was no significant change between room temperature and 600°C . When the total surface

area was separated into the surface areas attributable to intersplat pores and intrasplat cracks, different temperature dependencies were found. At temperatures between 600 and 1000°C the surface area of the cracks was found to decrease greatly, whereas the surface area of the intersplat pores changed hardly at all. Above 1000°C the intersplat pore surface area started to decrease.

These changes could be correlated with changes observed in the 3-D distributions of the apparent Porod surface areas, which showed a significant increase in the anisotropy associated with a selective reduction of the surface area attributable to cracks at lower temperatures (Figs. 4-6).

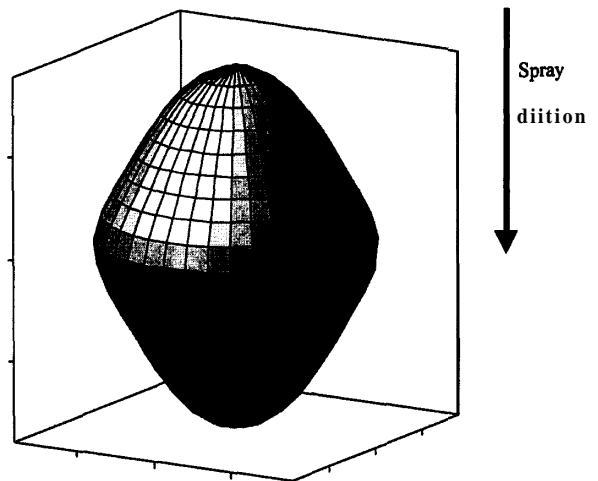


Fig. 4. Apparent Porod surface area distributions of the as-sprayed deposit. Note that on the axes in these figures is plotted the specific surface area, the 0 is in the middle and all three axes in each figure have the same scale. The values and labels are left out for clarity.

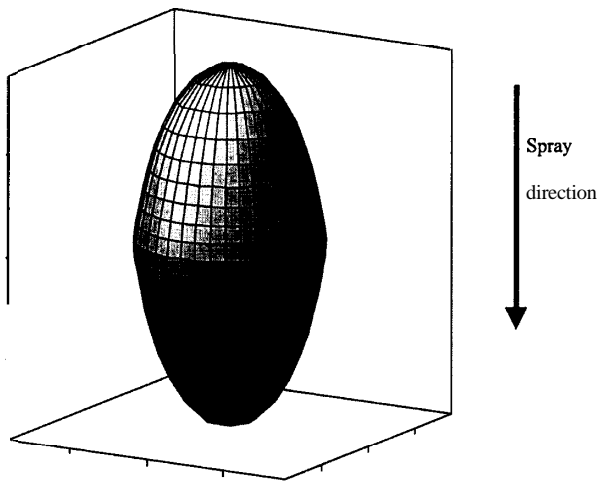


Fig. 5. Apparent Porod surface area distributions of the sample at 1100°C. Note that on the axes in these figures is plotted the specific surface area, the 0 is in the middle and all three axes in each figure have the same scale. The values and labels are left out for clarity.

The characteristic temperatures for surface area reduction in each void system were found (Fig. 3) assuming a sigmoidal dependence of the surface area on the temperature. The characteristic temperature for cracks was 870°C ($\pm 9^\circ\text{C}$) while that for intersplat pores was 1300°C ($\pm 50^\circ\text{C}$). These temperatures indicate for each system the temperature at which the rate of surface reduction is fastest. It should be noted that these temperatures must depend on the kinetics of the heating rate, and, thus, are likely to be different under different experimental conditions.

While the overall anisotropy of the void system changes significantly, the anisotropy of the apparent surface area distribution of the intersplat pore system does not change, remaining the same at all elevated

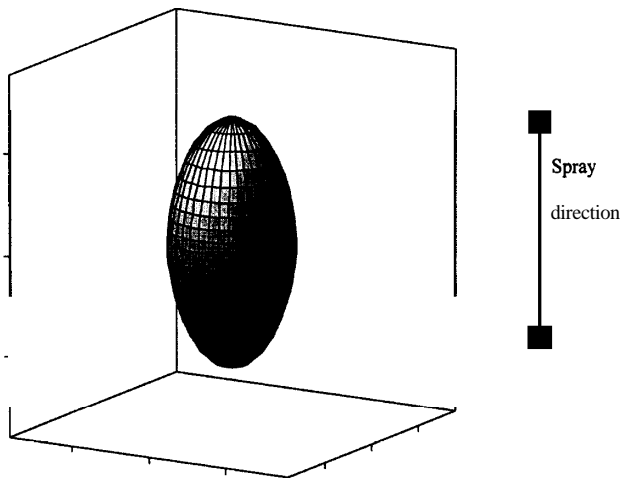


Fig. 6. Apparent Porod surface area distributions of the sample at 1400°C. Note that on the axes in these figures is plotted the specific surface area, the 0 is in the middle and all three axes in each figure have the same scale. The values and labels are left out for clarity.

temperatures as for the as-sprayed sample. Thus, the increase in the overall (prolate) anisotropy seems to be due entirely to the reduction in surface area of the crack population.

4. Discussion

The most important result from this study is that the total specific surface area of the void system decreased by about 33% from the as-sprayed condition when the deposit was heated below 1000°C. These are considered to be low temperatures relative to the operational environment. This result has important technical ramifications since it had not previously been determined because most characterizations of plasma sprayed deposits have been performed on as-sprayed deposits. The present results indicate that material processes are occurring at unexpectedly low temperatures, and that these processes cause a significant change in the microstructure.

The two anisotropic void systems in the plasma-sprayed deposit exhibit different behavior during annealing. The observed difference in effective annealing temperature was about 400°C under the conditions of the current experiment, but we acknowledge, that this temperature difference may be related to the experiment kinetics. The intersplat pore system surface area decreases at higher temperatures than does the surface area of the crack system. This phenomenon is likely related to the different sizes and shapes of the voids in each system, and, therefore, to different effective sintering temperatures. The origin of the shape and size differences likely lies in the different processes of void formation. Cracks probably result in rougher internal surfaces, as well as shapes which exhibit sharper angles. Intersplat pores form between the lamellae and already solidified splats, and thus have smoother surfaces which have never been closed. Sliding of splats during cooling may smooth these pore surfaces further.

As a result of crack sintering at lower temperatures, the structure with respect to the as-sprayed condition becomes more anisotropic, Figs. 5 and 6. The total surface area decreases at each of the temperatures examined and the dependence shown in Fig. 3 suggests that the reduction may continue to even higher temperatures than those studied.

The anisotropy in the intersplat pore system described by the aspect ratio of the apparent surface area distribution did not change in the temperature range studied. This suggests that the intersplat voids are closed during this type of experiment, but that they do not change their shape and orientation. Changes in shape (i.e. spheroidization) as well as changes in orientation (if any process is possible) would result in a change of anisotropy of their apparent Porod surface

area distribution. This important finding may help distinguish among processes that are active under these conditions.

5. Conclusions

Changes related to the sintering of the voids within plasma sprayed YSZ deposits have been observed at unexpectedly low temperatures; about 33% of the surface area in the as-sprayed condition is lost at temperatures below 1000°C. Thus, significant changes in the microstructure are occurring well below the normal operating temperatures of the coatings. The microstructure changes further in the normal operating temperature range of these coatings (between 1100 and 1250°C).

The microstructure was found to become more anisotropic below 1000°C. At higher temperatures, this anisotropy changed only a little. This effect can be attributed to the fact that the cracks sinter at lower temperatures than do the intersplat pores. The apparent surface area distribution of the intersplat pores retained its anisotropy at temperatures between 1000 and 1400°C.

Acknowledgements

This research was supported, in part, by the National Science Foundation MRSEC Program at the State University of New York at Stony Brook under Grant No. 9632570.

References

- [1] R. Sivakumar, B.L. Mordike, *Surf. Coat. Technol.* 37 (1989) 136.
- [2] R.A. Miller, *J. Therm. Spray Technol.* 6 (1) (1997) 35.
- [3] T.M. Yonushonis, *J. Therm. Spray Technol.* 6 (1) (1997) 50.
- [4] S. Bose, J. DeMasi-Marcin, *J. Therm. Spray Technol.* 6 (1) (1997) 99.
- [5] R.A. Miller, *Surf. Coat. Technol.* 30 (1987) 1.

- [6] S.M. Meier, D.K. Gupta, *J. Eng. Gas Turbines* 116 (1994) 250.
- [7] R.C. Novak, A.P. Matarese, R.P. Huston, A.J. Scharman, *Mater. Manuf. Process.* 7 (1) (1992) 15.
- [8] I. Kvernes, in: P. Vincenzini (Ed.), *High Tech Ceramics*, Elsevier, Amsterdam, 1987, pp. 361–394.
- [9] H.W. Grunling, W. Mannsmann, *J. Physique IV (Fr.)* 3 (1993) C7–903.
- [10] R.A. Miller, *J. Am. Ceram. Soc.* 67 (8) (1984) 517.
- [11] A. Levy, S. Macadam, *Surf. Coat. Technol.* 30 (1987) 51.
- [12] S.R. Levine, R.A. Miller, P.E. Hodge, *Sampe Q.* 12 (1) (1980) 20.
- [13] T. Cosack, L. Pawlowski, S. Schneiderbanger, S. Sturlese, *J. Eng. Gas Turbines Power* 116 (1994) 272.
- [14] J. Janata, P. Chraska, *Acta Tech. CSAV* 2 (1990) 223.
- [15] P.D. Harmsworth, R. Stevens, *J. Mater. Sci.* 27 (1992) 616.
- [16] H. Ibegazene, S. Alperine, C. Diot, *J. Mater. Sci.* 30 (1995) 938.
- [17] J. Ilavsky, H. Herman, C.C. Berndt, et al., in: C.C. Berndt, S. Sampath (Eds.), *Thermal Spray Industrial Applications*, ASM International, Materials Park, OH, 1994, pp. 709–714.
- [18] J. Ilavsky, G.G. Long, A.J. Allen, H. Herman, C.C. Berndt, in: C.C. Berndt (Ed.), *Thermal Spray: A United Forum for Scientific and Technological Advances*, ASM International, Materials Park, OH, 1997, pp. 697–702.
- [19] P. Bengtsson, T. Jonannesson, J. Wigren, in: A. Ohmori (Ed.), *Thermal Spraying-Current Status and Future Trends, Proceedings of the 14th International Thermal Spray Conference*, High Temperature Society of Japan, Osaka, Japan, 1995, pp. 513–518.
- [20] A. Ohmori, C. Li, *Thin Solid Films* 201 (1991) 241.
- [21] S. Kuroda, T.W. Clyne, *Thin Solid Films* 200 (1991) 49.
- [22] J. Ilavsky, A.J. Allen, G.G. Long, et al., in: A. Ohmori (Ed.), *Thermal Spraying-Current Status and Future Trends, Proceedings of the 14th International Thermal Spray Conference*, High Temperature Society of Japan, Osaka, Japan, 1995, pp. 483–488.
- [23] C.C. Berndt, *J. Mater. Sci.* 24 (1989) 3511.
- [24] J. Ilavsky, J.K. Stalick, in: C.C. Berndt (Ed.), *Thermal Spray: A United Forum for Scientific and Technological Advances*, ASM International, Materials Park, OH, 1997, pp. 691–695.
- [25] J. Ilavsky, A.J. Allen, G.G. Long, S. Krueger, C.C. Berndt, H. Herman, *J. Am. Ceram. Soc.* 80 (3) (1997) 733.
- [26] H.M. Kerch, H.E. Burdette, G.G. Long, *J. Appl. Cryst.* 28 (5) (1995) 604.
- [27] G. Kostorz, in: G. Kostorz (Ed.), *Treatise on Materials Science and Technology*, vol. 15, Academic Press, New York, 1979, pp. 227–290.
- [28] F.M. Hamzeh, R.H. Bragg, *J. Appl. Phys.* 45 (7) (1974) 3189.
- [29] W. Wu, *J. Polym. Sci. Polym. Phys. Ed.* 18 (1980) 1659.
- [30] J. Ilavsky, G.G. Long, A.J. Allen, H. Herman, C.C. Berndt, in: C.C. Berndt (Ed.), *Thermal Spray practical Solutions for Engineering Problems, Proceedings of 9th National Thermal Spray Conference*, ASM International, Materials Park, OH, 1996, pp. 725–728.